Molecular Cell
Article

XIAP Induces NF-κB Activation via the BIR1/TAB1 Interaction and BIR1 Dimerization

Miao Lu,[1] Su-Chang Lin,[1] Yihua Huang,[1,4] Young Jun Kang,[2] Rebecca Rich,[3] Yu-Chih Lo,[1] David Myszka,[3] Jiahuai Han,[2] and Hao Wu[1,*]
[1] Department of Biochemistry, Weill Medical College of Cornell University, New York, NY 10021, USA
[2] Department of Immunology, The Scripps Research Institute, La Jolla, CA 92037, USA
[3] Center for Biomolecular Interaction Analysis, School of Medicine, University of Utah, Salt Lake City, UT 84132, USA
[4] Present address: Department of Biochemistry, University of Texas Southwestern Medical Center, Dallas, TX 75390, USA.
*Correspondence: haowu@med.cornell.edu
DOI 10.1016/j.molcel.2007.05.006

SUMMARY

In addition to caspase inhibition, X-linked inhibitor of apoptosis (XIAP) induces NF-κB and MAP kinase activation during TGF-b and BMP receptor signaling and upon overexpression. Here we show that the BIR1 domain of XIAP, which has no previously ascribed function, directly interacts with TAB1 to induce NF-κB activation. TAB1 is an upstream adaptor for the activation of the kinase TAK1, which in turn couples to the NF-κB pathway. We report the crystal structures of BIR1, TAB1, and the BIR1/TAB1 complex. The BIR1/TAB1 structure reveals a striking butterfly-shaped dimer and the detailed interaction between BIR1 and TAB1. Structure-based mutagenesis and knockdown of TAB1 show unambiguously that the BIR1/TAB1 interaction is crucial for XIAP-induced TAK1 and NF-κB activation. We show that although not interacting with BIR1, Smac, the antagonist for caspase inhibition by XIAP, also inhibits the XIAP/TAB1 interaction. Disruption of BIR1 dimerization abolishes XIAP-mediated NF-κB activation, implicating a proximity-induced mechanism for TAK1 activation.

INTRODUCTION

The inhibitor of apoptosis proteins (IAPs) were originally identified in baculoviruses but have been subsequently found in diverse organisms (Crook et al., 1993; Duckett et al., 1996; Hay et al., 1995). They are characterized by the presence of conserved baculoviral IAP repeat (BIR) domains (Eckelman et al., 2006; Schimmer et al., 2006). In humans, the current IAP family members include X-linked inhibitor of apoptosis (XIAP), cIAP1, cIAP2, ML-IAP, NAIP, ILP2, Survivin, and Bruce (Eckelman et al., 2006). Although the first recognized function of IAPs is antiapoptosis and caspase inhibition, IAPs are now known as a family of multifunctional proteins that also play critical roles in receptor signaling, cell division, copper metabolism, and ubiquitination of proteins for proteasomal degradation (Eckelman et al., 2006; Mufti et al., 2006; Vaux and Silke, 2005).

XIAP is the best-studied member of the IAP family. It contains three BIR domains and a RING domain (Deveraux et al., 1997; Duckett et al., 1996; Holcik et al., 2001) (see Figure S1 in the Supplemental Data available with this article online). Previous structural and biochemical studies have shown that the linker preceding the BIR2 domain of XIAP directly blocks the active sites of caspase-3 and caspase-7 (Chai et al., 2001; Huang et al., 2001; Riedl et al., 2001), while the BIR3 domain sterically hinders caspase-9 dimerization and its activation (Shiozaki et al., 2003). By doing so, XIAP acts as a brake on caspase-mediated cellular dismantling. Upon apoptosis induction, Smac (also known as DIABLO) gets released from the intermembrane space of the mitochondria and interacts with the BIR2 and BIR3 domains of XIAP to relieve caspase inhibition (Chai et al., 2000; Du et al., 2000; Huang et al., 2003; Verhagen et al., 2000; Wu et al., 2000). The RING domain of XIAP may act as an E3 in the ubiquitination pathway to promote the turnover of a number of cellular proteins as well as itself (Vaux and Silke, 2005). The function of the BIR1 domain is unknown.

In addition to the well-characterized function of XIAP in caspase inhibition, an important function of XIAP is its role in signaling to NF-κB and MAP kinase activation (Birkey Reffey et al., 2001; Lewis et al., 2004; Sanna et al., 1998; Shibuya et al., 1996; Yamaguchi et al., 1995, 1999). In fact, while the caspase inhibitory function of XIAP does not appear to be conserved in other IAP family members (Eckelman et al., 2006), this signaling function of XIAP is conserved in at least two other IAP members, NAIP and ML-IAP (Sanna et al., 2002). In addition, two other IAPs, cIAP1 and cIAP2, associate with TRAFs in the TNF signaling pathway (Rothe et al., 1995) and may facilitate or

regulate TRAF-mediated NF-κB and MAP kinase activation (Tang et al., 2003).

Under physiological states, XIAP plays a role in development by mediating transforming growth factor β (TGF-b) and bone morphogenetic protein (BMP) signaling. It bridges the TGF-b and BMP type I receptors to TAK1 (Birkey Reffey et al., 2001; Yamaguchi et al., 1999). TAK1 is a MAP kinase kinase kinase (MAP3K) that activates MAP kinases and NF-κB transcription factors by directly activating MAP kinase kinase (MKK) and the inhibitor of κB kinase (IKK) (Wang et al., 2001; Yamaguchi et al., 1995). It is essential for mesoderm induction and patterning in early *Xenopus* development (Shibuya et al., 1996, 1998; Yamaguchi et al., 1995), for diverse developmental roles such as control of cell shape and regulation of apoptosis in *Drosophila* (Takatsu et al., 2000), and for vascular development in mice (Jadrich et al., 2003, 2006). Injection of XIAP mRNA into dorsal blastomeres enhanced the ventralization of *Xenopus* embryos in a TAK1-dependent manner (Yamaguchi et al., 1999), confirming the role of XIAP in development. Moreover, XIAP deficiency in mice exhibits delays in the development of the mammary gland in a manner that correlates with delayed NF-κB activation (Olayioye et al., 2005), suggesting that the role of XIAP in development is related to its TAK1 and NF-κB activation ability.

XIAP is differentially upregulated in many forms of human cancers and confers resistance to chemotherapy-induced cell death (Berezovskaya et al., 2005; Wilkinson et al., 2004). In contrast, downregulation of XIAP with siRNA or antisense oligonucleotides enhances sensitivity to chemotherapy for a variety of malignant cell lines (Chawla-Sarkar et al., 2004; McManus et al., 2004; Sasaki et al., 2000; Tong et al., 2005). XIAP is heavily pursued as a target for anticancer therapy, both by antisense oligonucleotides that target XIAP expression and by small molecules that disrupt protein-protein interactions in XIAP function (Andersen et al., 2005; Schimmer et al., 2006). The NF-κB activating function of XIAP may be important for cancer cell survival under these pathological conditions. In support of this, it has been shown that the anti-apoptotic activity of XIAP is dependent on TAK1-mediated survival signaling (Lewis et al., 2004; Sanna et al., 1998, 2002) and that XIAP-mediated TAK1-dependent NF-κB activation is important for endothelial cell survival (Hofer-Warbinek et al., 2000; Levkau et al., 2001).

The molecular mechanism of XIAP-mediated TAK1 activation has been a subject of debate. A yeast two-hybrid screen has shown that the region of XIAP comprising the three BIR domains interacts with the N-terminal domain of the TAK1 binding protein TAB1 (Yamaguchi et al., 1999), suggesting that XIAP activates TAK1 via TAB1. However, it has also been suggested that XIAP directly interacts with TAK1 (Sanna et al., 2002) and that the RING domain of XIAP acts as an E3 in nondegradative ubiquitination for NF-κB activation (Lewis et al., 2004). To resolve these conflicting issues, we performed a series of biochemical, structural, and cell biological experiments. We showed that the BIR1 domain of XIAP, which has no previously ascribed function, interacts specifically with TAB1. We determined the crystal structure of the BIR1/TAB1 complex, as well as the structures of isolated BIR1 and TAB1. Revelation of the BIR1/TAB1 interface allowed us to rigorously determine whether XIAP-induced TAK1 activation is through TAB1. An XIAP construct that contains the BIR domains only efficiently induced TAK1 and NF-κB activation. Structure-based mutations that disrupt TAB1 interaction and siRNA-mediated knockdown of TAB1 showed that the BIR1/TAB1 interaction is crucial for XIAP-induced TAK1 and NF-κB activation. We further showed that despite its not directly interacting with BIR1, Smac, the antagonist for caspase inhibition by XIAP, also inhibited the XIAP/TAB1 interaction.

What is the molecular mechanism of XIAP-TAB1-induced TAK1 activation? It was proposed recently based on the crystal structure of TAB1 that TAB1 is a pseudo-phosphatase bearing the fold of protein phosphatase type 2C (PP2C) and likely binds to and regulates accessibility of phosphorylated residues on substrates downstream of TAK1 or on the TAK1 complex itself (Conner et al., 2006). Our structure of TAB1 alone is highly similar to the reported structure, but our structural analysis suggests that TAB1 cannot bind phosphates due to the mutation of a crucial Arg to Ser, incomplete metal ion binding, and excess negative charge at the active site. Instead, our structure revealed a dimerization tendency of the BIR1 domain of XIAP both in the crystals and in solution. We showed that disruption of XIAP dimerization abolished XIAP-mediated NF-κB activation.

Therefore, our study revealed the molecular mechanism of XIAP-induced TAK1 and NF-κB activation and may provide a new target for anticancer therapy. The molecular mechanism identified here may also have general implications for TAK1 activation in other signaling systems.

RESULTS

The BIR1 Domain of XIAP Is Sufficient for TAB1 Interaction

To determine which BIR domain of XIAP is responsible for TAB1 interaction, we first used native PAGE band shift assay to dissect this interaction. Surprisingly, the BIR1 domain, which has no previously ascribed function, is the only BIR domain that interacted with the N-terminal domain of TAB1. This interaction was confirmed by comigration of BIR1 and TAB1 on gel filtration chromatography (Figure 1A). We further used surface plasmon resonance (SPR) to quantitatively determine whether BIR1 is sufficient for TAB1 interaction. The measurements showed that BIR1 and BIR1-3 of XIAP have similar affinity for TAB1 (Table 1, Figures 1B and 1C), demonstrating that BIR1 is sufficient for TAB1 interaction.

Structure Determination

We determined the crystal structures of BIR1 at 1.8 Å resolution using single wavelength anomalous diffraction of

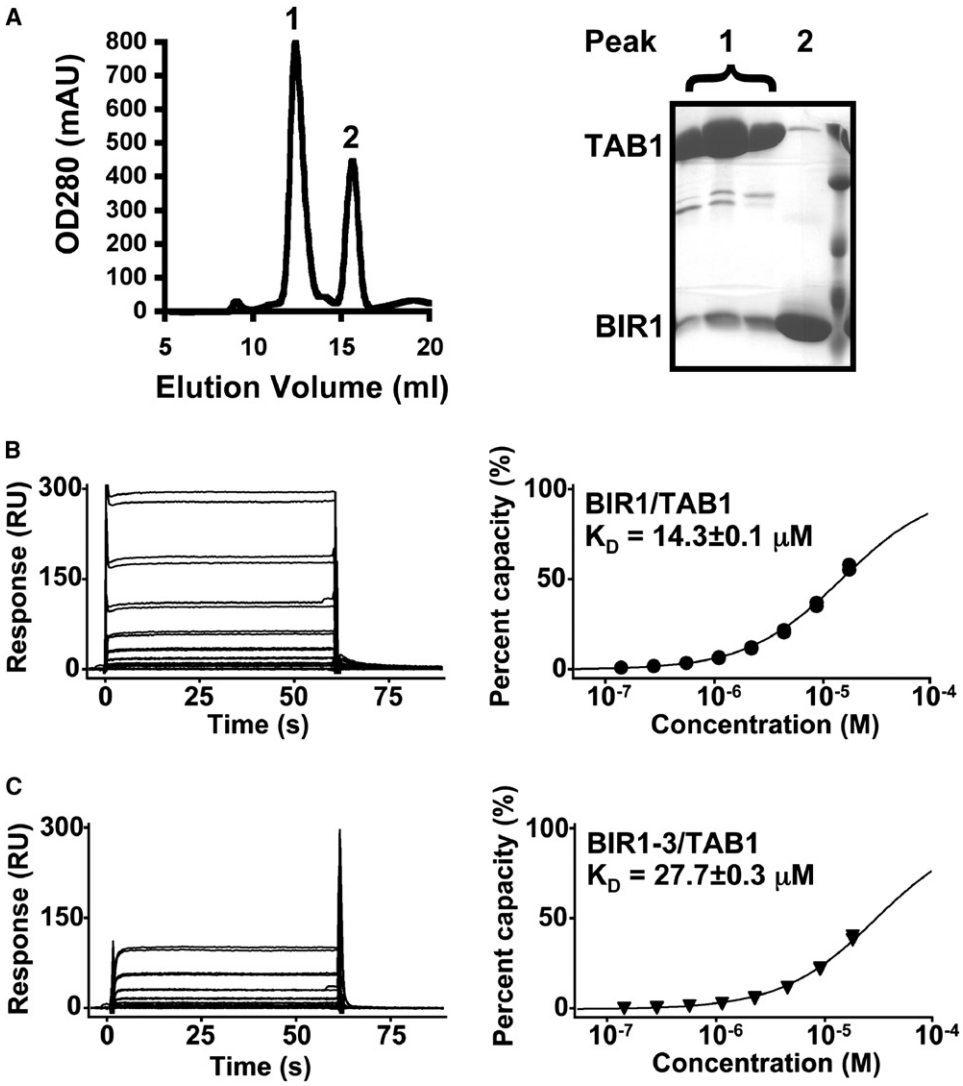

Figure 1. Biochemical Analysis of the Interaction between the BIR1 Domain of XIAP and the N-Terminal Domain of TAB1

(A) Comigration of BIR1 and TAB1 N-terminal domain on gel filtration chromatography.

(B) Duplicate responses (left) and isotherms (right) for a 2-fold dilution series (0.143–18.25 μM) of TAB1 binding to surface-tethered BIR1 in an SPR experiment.

(C) Duplicate responses (left) and isotherms (right) for a 2-fold dilution series (0.143–18.25 μM) of TAB1 binding to surface-tethered BIR1-3 in an SPR experiment.

its intrinsic zinc, the N-terminal domain of TAB1 at 2.4 Å resolution from a three wavelength anomalous diffraction data set of its selenomethionyl crystal, and the BIR1/TAB1 complex at 3.1 Å resolution by molecular replacement (Table 1). The TAB1 structure has the fold of mammalian PP2Cα, but with a unique helical extension (Figure 2A) (Conner et al., 2006). To facilitate crystallization of the BIR1/TAB1 complex, we used an internal deletion mutant of TAB1 (TAB1D, Δ133–151) without this unique helical extension domain. This deletion did not affect its ability to interact with BIR1 or BIR1-3 of XIAP (Table 1).

BIR1 and TAB1 Form an Extensive and Specific Interface

There are two independent copies of the BIR1/TAB1 complex in the asymmetric unit of the crystal. The two complexes are almost identical with a superimposed RMSD of 0.4 Å, suggesting a specific interaction between BIR1 and TAB1. No significant structural changes are observed in TAB1 before and after BIR1 binding or as a result of deletion of the helical extension domain.

The two BIR1/TAB1 complexes form an almost perfect noncrystallographic dimer (176° rotation, Figure 2B). The

Table 1. Surface Plasmon Resonance and Crystallographic Statistics

SPR	K_D (μM)		K_D (μM)
BIR1-3/TAB1	27.7 ± 0.3	BIR1-3/TAB1D[1]	16.1 ± 0.2
BIR1/TAB1	14.3 ± 0.1	BIR1/TAB1D[1]	4.2 ± 0.2
Crystallography	TAB1	BIR1	BIR1/TAB1D[1]
Constructs	Residues 1–370	Residues 20–99	Residues 10–99 of BIR1; TAB1D[1]
Structure Determination	MAD	SAD	MR
Data Collection			
Beamlines	X4A of NSLS	X4A of NSLS	X4C of NSLS
Space group	P321	I222	$P2_12_12_1$
Cell dimensions a, b, c (Å)	143.4, 143.4, 66.1	34.9, 73.0, 81.7	61.0, 108.7, 175.7
Resolution	30–2.4 Å	30–1.8 Å	30–3.1 Å
R_{sym}	6.4% (27.8%)	5.5% (18.3%)	13.0% (47.7%)
I/σI	27.8 (4.2)	11.9 (2.5)	10.0 (3.2)
Completeness	98.6% (95.9%)	92.6% (66.0%)	82.4% (66.0%)
Redundancy	4.5 (3.1)	3.6 (2.1)	4.3 (2.5)
Refinement			
Resolution	30–2.5 Å	30–1.8 Å	30–3.1 Å
Number of reflections	26,191	16,989	16,920
R_{work}/R_{free}	21.4%/24.9%	20.3%/21.3%	21.5%/29.3%
Number of atoms			
Protein	2733	614	6268
Water and ion	65	86	2
Average B factors			
Protein	53.2 $Å^2$	28.3 $Å^2$	77.1 $Å^2$
Water and ion	42.6 $Å^2$	39.5 $Å^2$	80.6 $Å^2$
Rmsds			
Bond lengths/angles	0.009 Å/1.47°	0.007 Å/1.23°	0.007 Å/1.33°
Ramachandran plot			
Most favored/allowed	90.1%/9.9%	90.9%/9.1%	70.1%/26.0%

Highest resolution shell is shown in parentheses.
[1] TAB1D, residues 1–370 with deletion of residues 133–151.

dimer resembles the shape of a butterfly, with the two BIR1 molecules as the body and the two TAB1 molecules as the wings. The interaction between BIR1 and TAB1 is extensive, burying ~1400 $Å^2$ surface areas at each interface (Figure 2C). There are a total of 121 pairs of Van der Waals interactions, which are mixed with both hydrophobic and hydrophilic contributions.

BIR1 and TAB1 exhibit shape complementarity with the concave surface of BIR1 receiving the convex surface of TAB1 (Figure 2D). The region of TAB1 involved in BIR1 interaction resides at the back side of the TAB1 structure (Figures 2A and 2C). This region includes residues mainly from α2, α3, and β9 (Figures 2A and 3A). Based on surface area burial, residues D213 and F216 of TAB1 contribute most to the interaction. Residues of BIR1 involved in TAB1 interaction reside at α2 and α3 and loops preceding them and after α4 (Figure 3B). Based on surface area burial, residues Y75, V80, and L98 contribute most to the interaction.

A number of hydrogen bonding interactions are observed at the BIR1/TAB1 interface (Figure 2C). These include an ion pair between E212 of TAB1 and R84 of BIR1, hydrogen bonds between the carboxylate of D213 of TAB1 and the amide nitrogens of A79 and V80 of BIR1, hydrogen bonds between the carboxylate of E271 of TAB1 and the side-chain hydroxyls of S43 and T46 of BIR1, and a side-chain hydrogen bond between Q276 of TAB1 and Y75 of BIR1. Residues at the BIR1/TAB1 interface are mostly conserved across species (Figure 3), suggesting that the interaction is preserved through evolution.

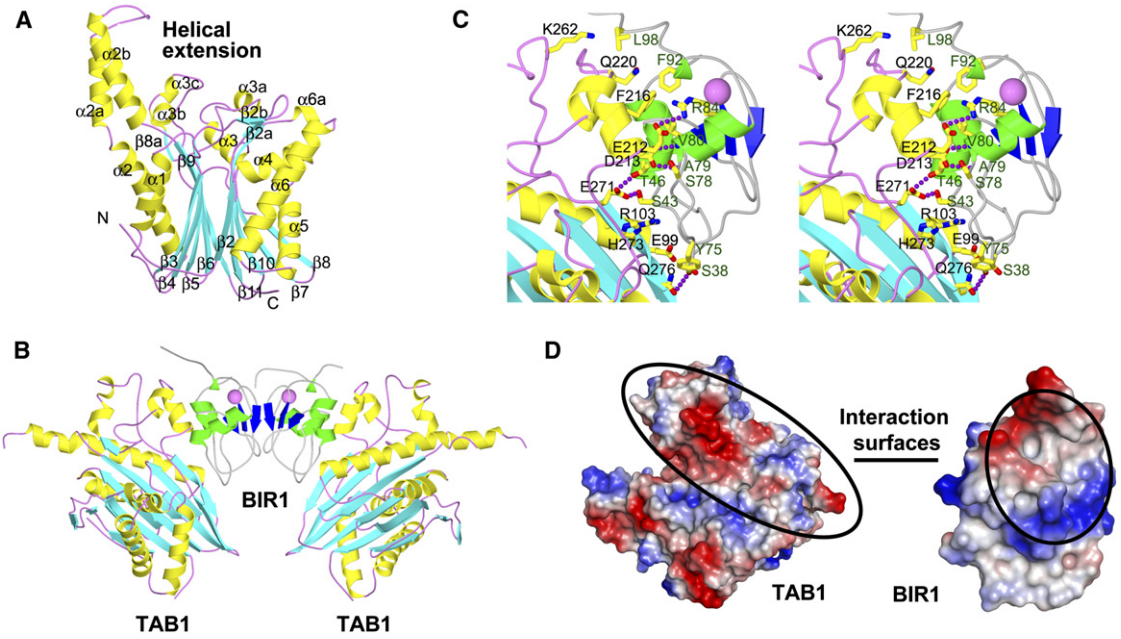

Figure 2. Structural Analysis of the Interaction between the BIR1 Domain of XIAP and the N-Terminal Domain of TAB1

(A) A ribbon diagram of TAB1. Helices, β strands, and loops are shown in yellow, cyan, and pink, respectively.

(B) Dimeric BIR1/TAB1 complex. TAB1 is shown with helices in yellow, β strands in cyan, and loops in pink, respectively. BIR1 is shown with helices in green, β strands in blue, and loops in gray.

(C) A stereo diagram for the detailed interaction between BIR1 and TAB1. Interface residues and their hydrogen bonding interactions are labeled.

(D) Electrostatic surfaces of BIR1 and TAB1, showing the charge and shape complementarity.

In contrast, these residues show poor conservation among PP2Cα and PstP, suggesting that BIR1 interaction is a unique property of TAB1.

The BIR2 and BIR3 domains of XIAP have been shown to interact with the Smac dimer (Huang et al., 2003; Wu et al., 2000). The surface of BIR1 equivalent to the Smac interaction surface of BIR2 and BIR3 is opposite to its TAB1 binding surface. In contrast, the dimerization surface of BIR1 overlaps with the equivalent Smac binding surface of BIR2 and BIR3 (see below).

The BIR1/TAB1 Interaction Is Crucial for XIAP-Induced NF-κB Activation

We performed extensive structure-based mutagenesis on the BIR1/TAB1 interaction. TAB1 mutants D213A and F216A both completely abolished the ability of TAB1 to interact with BIR1 (Figure 3C). Single site mutations of BIR1, including Y75G, V80A, and L98G, did not completely eliminate the ability of BIR1 to interact with TAB1. In contrast, V80D, which introduces a negative charge to the interface, eliminated the ability of BIR1 to interact with TAB1 (Figure 3C). Double mutations of any combination on these residues of BIR1 or the triple mutation also completely knocked out the interaction (Figure 3C).

To determine whether the BIR1/TAB1 interaction is critical for XIAP-induced TAK1 activation, we introduced the TAB1-binding disruptive mutation V80D and the TAB-1-binding reduced mutant V80A into the mammalian expression construct of XIAP containing the BIR1-3 domains. We transfected wild-type (WT) and mutant XIAP into 293T cells and determined their ability to activate NF-κB, the downstream effector of TAK1 activation (Figure 4A). While WT XIAP efficiently induced NF-κB activation, the V80D and the V80A mutants of XIAP exhibited reduced ability to activate NF-κB. The effect of the V80A mutant is less drastic than the V80D mutant, consistent with the residual ability of V80A to binding TAB1 (Figures 3C and 4A). In addition, XIAP constructs with and without the RING domain induced similar levels of NF-κB activation, suggesting that the RING is not critical for XIAP-induced signaling in these cells.

To determine whether the reduced ability of XIAP mutants to activate NF-κB is due to impaired TAK1 activation, we performed in vitro kinase assay on immunoprecipitated TAK1 in XIAP transfected cells (Figure 4B). While WT full length or BIR1-3 of XIAP efficiently induced TAK1 activation as shown by the phosphorylation of the TAK1 substrate MKK6, the V80D and the V80A mutants exhibited much reduced TAK1 activation. Consistent with the degree of defectiveness in TAB1 interaction, the V80D mutant showed the most drastic impairment in TAK1 activation.

To further demonstrate that TAB1 is responsible for XIAP-mediated NF-κB activation, we transfected the BIR1-3 domain of XIAP into two independent cultures of primary MEFs in which TAB1 has been knocked down using two different siRNA constructs (Kang et al., 2006).

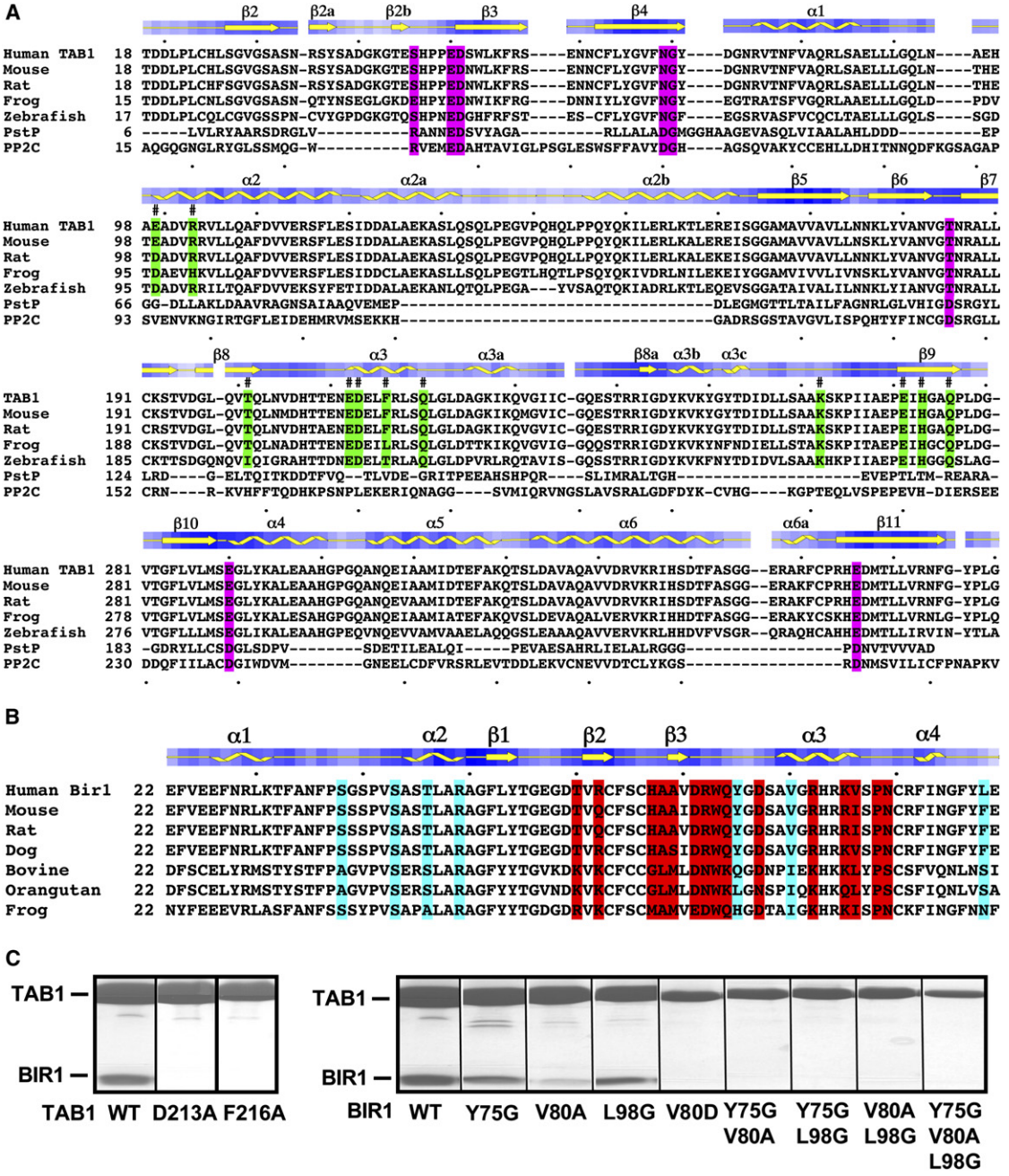

Figure 3. Structure-Based Sequence Alignment

(A) Alignment of TAB1, PP2Cα, and PstP. Secondary structures of TAB1 are labeled. Residues at the interface with BIR1 are highlighted in green, and residues at the active site of PP2C-like domains are highlighted in magenta.

(B) Alignment of BIR1 from different species. Secondary structures of BIR1 are labeled. Residues at the interface with TAB1 are highlighted in cyan, and residues at the dimerization interface are highlighted in red.

(C) Structure-based mutagenesis on the BIR1/TAB1 interaction, showing the peak fractions of gel filtration chromatography on TAB1 with WT and mutant BIR1.

Western blots and semiquantitative PCR confirmed the much-reduced expression of TAB1 for both siRNA constructs (Figure 4C). XIAP exhibited much reduced ability to activate NF-κB in both these cells in comparison with its effect in control MEFs (Figure 4C). This demonstrates that the BIR1/TAB1 interaction is crucial for XIAP-induced TAK1 activation and argues against direct association of XIAP with TAK1 as the means of TAK1 activation.

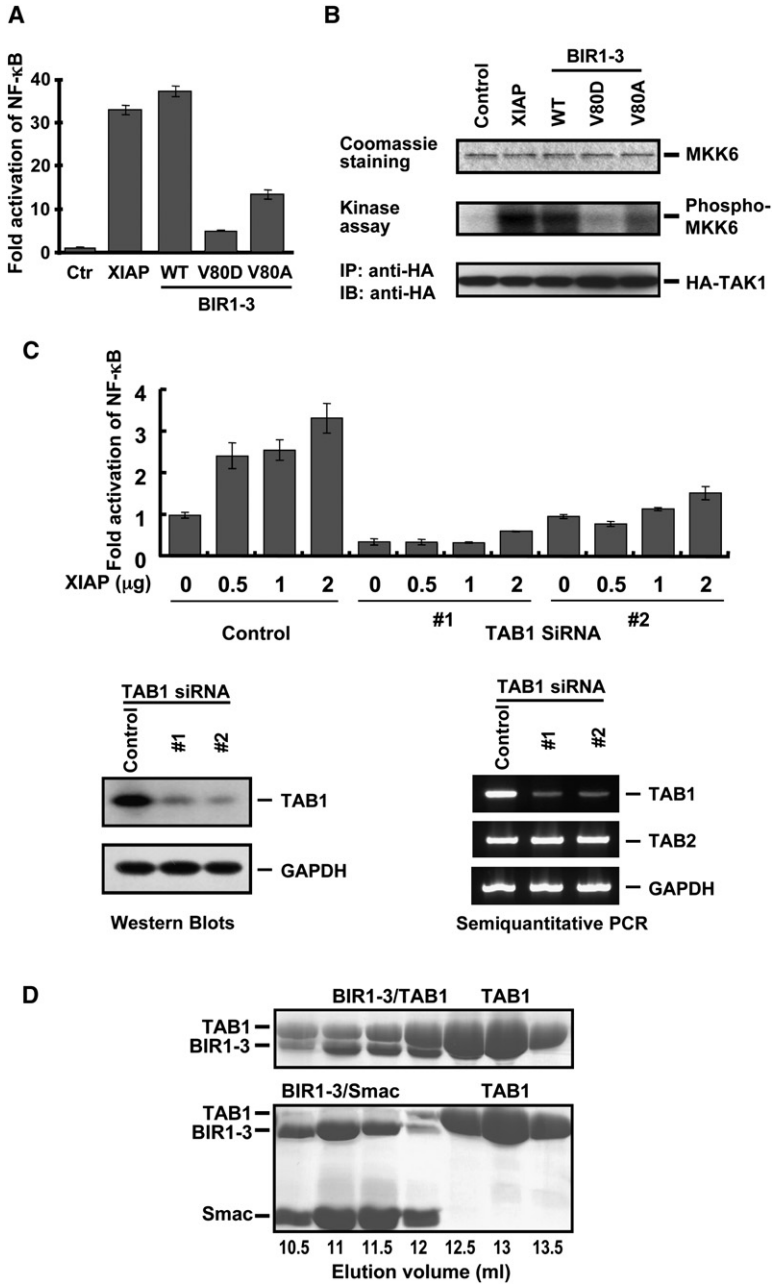

Figure 4. XIAP/TAB1 Interaction Is Critical for XIAP-Induced NF-κB Activation

(A) Defective and weakened NF-κB activation by the BIR1-3 mutant V80D and V80A.

(B) Defective and weakened TAK1 activation by the BIR1-3 mutant V80D and V80A.

(C) Defective NF-κB activation by BIR1-3 of XIAP in MEFs with siRNA-mediated TAB1 knockdowns.

(D) Smac inhibits XIAP/TAB1 interaction as shown by gel filtration.

In (A) and (C), error bars are mean standard deviations of duplicate samples and are representative of three independent experiments.

Although Smac Does Not Interact with BIR1, It Antagonizes the XIAP/TAB1 Interaction via Steric Exclusion

Because the caspase inhibitory function of XIAP is antagonized by Smac, a mitochondrial protein that gets released during apoptosis, we wondered whether Smac may also inhibit the XIAP/TAB1 interaction and therefore the signaling function of XIAP. We have shown previously that the Smac dimer interacts simultaneously with BIR2 and BIR3 domains of XIAP (Huang et al., 2003). This interaction excludes the interaction of the linker of XIAP, which resides before the BIR2 domain, with caspase-7 or caspase-3. To determine whether Smac also antagonizes the XIAP/TAB1 interaction, we used gel filtration to determine complex formation. While XIAP BIR1-3 comigrated with TAB1, this interaction was abolished in the presence of Smac (Figure 4D), demonstrating that Smac inhibits the interaction between TAB1 and XIAP. Therefore, Smac also antagonizes the ability of XIAP to activate TAK1 and regulates XIAP via several different mechanisms.

Because Smac does not interact with BIR1 (Liu et al., 2000; Wu et al., 2000), antagonizing XIAP/TAB1

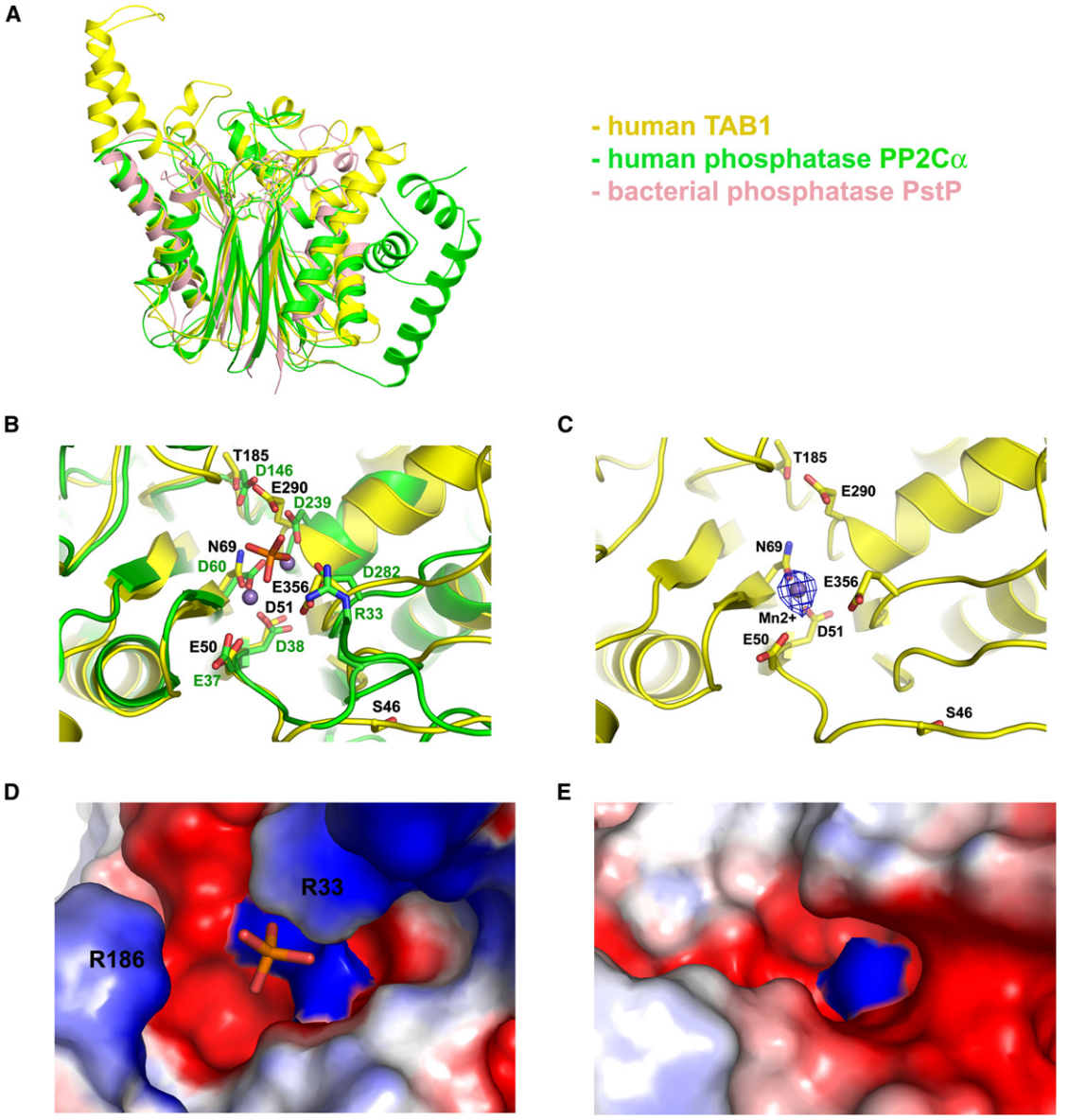

Figure 5. TAB1 Does Not Have Phosphatase Activity

(A) Superposition of human TAB1 (yellow), human phosphatase PP2Cα (green), and bacterial phosphatase PstP (pink).

(B) Superposition of the active sites of TAB1 (yellow) and PP2Cα (green). Two metal ions and one phosphate ion are bound at the PP2Cα active site. Residues important for metal ion coordination and catalysis are labeled in black for TAB1 and green for PP2Cα.

(C) Only one Mn^{2+} ion is bound at the TAB1 active site when soaked with $MnCl_2$. The $F_o - F_c$ map is shown at 10σ level.

(D) Electrostatic surface of the PP2Cα active site. The location of the bound phosphate ion is shown.

(E) Electrostatic surface of the same region in TAB1.

interaction by Smac is likely a result of steric exclusion, rather than direct competition. In this steric exclusion, simultaneous binding of the BIR2 and BIR3 domains of XIAP with the Smac dimer sterically prevents the binding of the BIR1 domain of the same XIAP molecule to TAB1. In support of this, a synthetic dimeric Smac peptide dAVPI did not inhibit the XIAP/TAB1 interaction (data not shown).

TAB1 Can Neither Catalyze Dephosphorylation nor Bind Phosphates

Like human PP2Cα (Das et al., 1996) and the bacterial phosphatase PstP (Pullen et al., 2004), the structure of TAB1 has the fold of PP2C-like domains with a central β sheet flanked by α helices at either side (Figures 2A and 5A). Catalysis by PP2Cs requires a two-metal binding center (Mg^{2+} or Mn^{2+}) at the active site, localized within the top

channel of the β sandwich (Das et al., 1996) (Figures 2A, 5A, and 5B). For human PP2Cα, Mn^{2+} stimulates its activity with a lower K_m than Mg^{2+}, although the physiological metal ion for catalysis is likely to be Mg^{2+} (Pato and Kerc, 1991). In the crystal structure of PP2Cα, the Mn^{2+} at site 1 directly contacts three Asp residues, D60, D239, and D282. The Mn^{2+} at site 2 only directly interacts with one Asp residue, D60. Other ligands for this metal include the carbonyl oxygen of G61 and three water molecules, two of which are stabilized by interactions with E37 and D38. In TAB1, D60, D239, and D282 of PP2Cα are changed to N69, E290, and E356, respectively, while E37, D38, and G61 of PP2Cα are conserved (Figures 3A and 5B). Another conserved Asp, D146 of PP2Cα, which coordinates a third metal ion near the active site in the bacterial phosphatase PstP and may enhance catalysis (Pullen et al., 2004), is changed to Thr in TAB1 (Figures 3A and 5B). Lack of a complete active site suggests that TAB1 does not have phosphatase activity, a conclusion that is also supported experimentally using artificial substrates (Conner et al., 2006 and data not shown).

It has been proposed that TAB1 may be a pseudophosphatase, possibly binding to phosphorylated residues on TAK1 or other molecules in the pathway and regulating their activity (Conner et al., 2006). However, phosphate binding, as shown in the PP2Cα structure, requires water molecules bound to both metal ions and a crucial Arg residue R33 (Das et al., 1996). In TAB1, R33 is changed to a Ser residue, S46 (Figures 3A and 5B). In addition, soaking of $MnCl_2$ into the crystals showed that only one Mn^{2+} is bound (Figure 5C). This Mn^{2+} corresponds to the PP2Cα ion 2. Furthermore, the two mutated metal-coordinating negatively charged surface residues, E290 and E356 of TAB1, are not coordinating any metals. Electrostatic surface calculations showed while PP2Cα active site is highly positively charged, the same region of TAB1 is largely negatively charged with the exception of the single metal ion surface (Figures 5D and 5E). Variation in the phosphate binding residue, lack of a metal ion, and excess negative charges strongly suggest that TAB1 cannot bind phosphates or phosphorylated residues.

BIR1 Dimerization Is Crucial for XIAP-Induced NF-κB Activation

The lack of phosphatase activity of TAB1 makes it unlikely that TAB1 directly regulates the phosphorylation state of TAK1 and thereby activates TAK1. In contrast, the dimeric assembly of the BIR1/TAB1 structure in the crystal prompted us to speculate that dimerization of BIR1 may lead to proximity-induced TAK1 activation. Interestingly, the same BIR1 dimer in the dimeric BIR1/TAB1 complex is also observed in the BIR1 crystal lattice in the absence of TAB1 (Figure 6A). This dimerization is mediated by mutual interactions among R62, D71, R72, D77, R82, K85, and V86, in which V86 is completely buried at the interface (Figure 6B). This dimerization interface of BIR1 is equivalent to the Smac interacting surfaces of BIR2 and BIR3.

To determine whether BIR1 has a tendency to dimerize in solution, we performed dynamic light scattering measurements at BIR1 concentrations from 10 mg/ml and up (Figure 6D). The calculated molecular weight of monomeric BIR1 is 10.5 kDa. The apparent molecular mass of BIR1 increased significantly as a function of concentration, to approximately dimeric at 30 mg/ml, suggesting that BIR1 does have a tendency to dimerize in solution. Similar dynamic light scattering measurements have also been used previously to assess dimerization tendency of human CD4 (Wu et al., 1997).

To determine whether this dimerization is important for XIAP-induced TAK1 activation, we mutated V86 to Glu to introduce a buried negative charge at the dimerization interface. While the V86E mutant retained its ability to interact with TAB1 (Figure 6C), its dimerization tendency was abrogated as shown by dynamic light scattering measurements (Figure 6D). Remarkably, upon transfection, the mutant XIAP also had much reduced ability to activate NF-κB (Figure 6E), demonstrating that XIAP dimerization is important for TAK1 activation and its associated biological effects. As a control, the TAB1 binding defective XIAP mutant V80D also showed decreased NF-κB activation.

DISCUSSION

Establishment of the XIAP-TAB1-TAK1 Pathway for XIAP-Mediated NF-κB Activation

The multifunctional IAP family member XIAP participates in diverse cellular functions including caspase inhibition, signal transduction, copper metabolism, and ubiquitination. For the signaling function, XIAP bridges TGF-b and BMP type I receptors to TAK1 and NF-κB activation under physiological conditions and induces survival signaling in cancer cells under pathological conditions. Here we establish that XIAP activates TAK1 via interaction with the TAK1 binding protein TAB1. While the RING domain of XIAP has been shown to interact with the receptors, we mapped the TAB1-interacting region of XIAP to the BIR1 domain. The affinity of XIAP or BIR1 with TAB1 is similar to several bona fide interactions involved in signal transduction such as the SH3-peptide and SH2-peptide interactions (Ferreon and Hilser, 2004).

The N-terminal domain of TAB1 interacts with BIR1 of XIAP, and the C-terminal tail of TAB1 interacts with the kinase domain of TAK1 (Figure 6F). Under endogenous conditions, TAB1 and TAK1 are constitutively associated with each other without TAK1 activation (Wang et al., 2001). In the crystal structure of a fusion protein containing the TAK1 kinase domain and the C-terminal tail of TAB1, TAB1 interacts with the C-terminal lobe of TAK1 (Brown et al., 2005). This interaction is similar to the binding of the myristoylated N terminus with the c-Abl kinase domain and presumably induces conformational changes in the kinase domain (Nagar et al., 2003). However, this interaction does not appear to directly lead to kinase activation as the fusion kinase is not phosphorylated at the crucial residues of the active site loop (Brown et al., 2005).

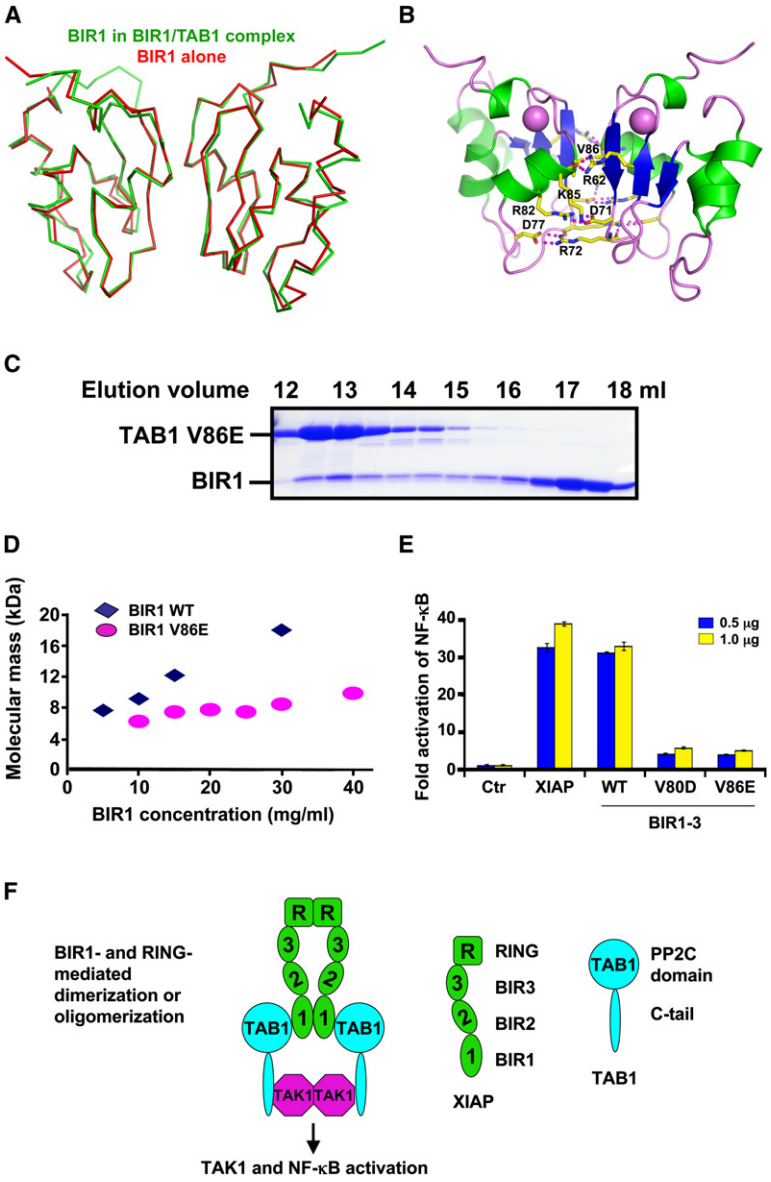

Figure 6. BIR1 Dimerization Is Critical for XIAP-Mediated NF-κB Activation

(A) Superposition of the BIR1 dimer in the crystal of BIR1 alone (red) and in complex with TAB1 (green).

(B) Dimerization interface of BIR1, showing important residues and their hydrogen bonding interactions.

(C) V86E mutant of BIR1 still interacts with TAB1 as shown by gel filtration.

(D) Apparent molecular mass of BIR1 WT and V86E mutant as a function of concentration as measured by dynamic light scattering.

(E) Defective NF-κB activation by the V86E mutant. The TAB1 binding defective mutant V80D was used as a control. Error bars are mean standard deviations of duplicate samples and are representative of three independent experiments.

(F) A schematic model for XIAP-mediated TAK1 and NF-κB activation.

Consistent with this hypothesis, the myristate-bound c-Abl kinase is also not active (Nagar et al., 2003).

The current study suggests that during TGF-b and BMP signaling or upon XIAP upregulation, XIAP interacts with TAB1 and brings the associated TAK1 into proximity for transphosphorylation and activation. Previous studies have suggested the involvement of XIAP RING domain in XIAP oligomerization and a residual self-association ability of RING-deleted XIAP (Silke et al., 2002, 2005). The ability of the RING domain to mediate XIAP oligomerization may be the reason for its requirement in signaling in some situations (Lewis et al., 2004). Therefore, it appears that while the RING domain may make XIAP a constitutive oligomer, the BIR1 domain mediates a specific and dynamic dimerization for TAK1 activation (Figure 6F).

Because XIAP is highly upregulated in many cancer cells (Schimmer et al., 2006), the high expression level in these cells may facilitate TAK1 activation by XIAP and contribute to the effect of XIAP in promoting cancer cell survival. The current study may provide a new target for suppressing XIAP function in cancer cells.

BIR1 as a General Mediator of Signaling and Dimerization

To our knowledge, this is the first time that any function of XIAP has been ascribed to the BIR1 domain, which is highly conserved across species. One surface of BIR1 is used for TAB1 interaction while the opposite surface, which is equivalent to the Smac binding surface of BIR2 and BIR3, is used for BIR1 dimerization.

In this context, it is interesting to note that the BIR1 domain of two other IAP family members, cIAP1 and cIAP2, has also been shown recently to mediate signaling and dimerization (Samuel et al., 2006; Varfolomeev et al., 2006; Zhou et al., 2005). The BIR1 domain of cIAP1 and cIAP2 mediates the interaction with TRAF1 and TRAF2, the major signaling proteins in intracellular signal transduction of TNF receptors (Samuel et al., 2006; Varfolomeev et al., 2006). In the most frequent chromosomal translocation associated with MALT lymphomas, the c-IAP2 BIR domains are fused with the paracaspase MALT1, resulting in constitutive cIAP2-MALT1 oligomerization and NF-κB activation. The BIR1 domain, but not BIR2 or BIR3 of cIAP2, mediates the oligomerization of the cIAP2-MALT1 fusion protein and is required for NF-κB activation (Zhou et al., 2005). Oligomerization and TRAF interaction of cIAPs are apparently mediated by different surfaces of BIR1 as the TRAF binding mutants of cIAP2-MALT1 still oligomerize and activate NF-κB (Varfolomeev et al., 2006). In the cIAP2-MALT1 fusion, cIAP2 appears to provide the oligomerization ability of the protein while MALT1 recruits other proteins for NF-κB activation (Zhou et al., 2005).

Broad Biological and Mechanistic Implications

Unlike the caspase inhibitory function, the signaling function of XIAP is conserved in several other IAPs such as NAIP and ML-IAP. These IAPs may also induce TAK1 activation via a similar TAB1-mediated mechanism.

TAK1 also plays a much broader role in survival signaling by acting as the upstream kinase for NF-κB and MAP kinase activation in multiple receptor signaling pathways including IL-1 receptor, Toll-like receptors, some TNF receptors, and antigen receptors (Chen, 2005; Deng et al., 2000; Wang et al., 2001). In these pathways, the signaling protein TRAF6 acts as an E3 to mediate nondegradative K63-linked polyubiquitination of itself and of downstream targets. Instead of TAB1, the TAK1 binding adaptor protein TAB2 (or its related protein TAB3) links TRAF6 to TAK1 (Kanayama et al., 2004; Takaesu et al., 2000). In this TRAF6-TAB2-TAK1 pathway, ubiquitination of TRAF6 promotes TAB2 recruitment and TAK1 activation. Because TRAF6 is induced to trimerize or form other oligomers upon receptor stimulation (Park et al., 1999; Ye et al., 2002), the current study implicates a general oligomerization-dependent mechanism for TAK1 activation in these diverse TAK1 and NF-κB activation pathways.

EXPERIMENTAL PROCEDURES

Protein Preparation and Mapping of the XIAP/TAB1 Interaction

Human XIAP deletion mutants (BIR1, residues 20–99; BIR2, residues 124–256; BIR3, residues 257–336; BIR1-3, residues 1–336), human TAB1 N-terminal domain (residues 1–370), and TAB1D (residues 1–370 with deletion of 133–151) were expressed as GST fusion proteins in bacteria, purified using glutathione beads, and cleaved with thrombin to remove the GST tag. The cleaved proteins contain two additional residues GS at the beginning of the proteins. Human BIR1 (residues 10–99) was expressed as an N-terminally His-tagged protein and purified by Ni-affinity chromatography. The tag was cleaved off by thrombin treatment. Smac was expressed and purified as described previously (Chai et al., 2000; Huang et al., 2003). For mapping studies, purified XIAP and TAB1 constructs were mixed, incubated, and subject to native PAGE using the PhastSystem (GE Biosciences) and gel filtration using Superdex 200 HR 10/30 (GE Biosciences).

Surface Plasmon Resonance Measurements

Binding studies were performed at 20°C using a Biacore 2000 optical biosensor equipped with a streptavidin-coated CM4 research-grade sensor chip and equilibrated with running buffer (20 mM Tris, 75 mM NaCl, 0.005% P20, and 0.1 mg/ml BSA [pH 8.0]). BIR1 and BIR1-3 of XIAP were incubated with EZ-link sulfo-NHS-LC-LC-biotin for 1 hr, passed over a fast desalting column to remove free biotin, and captured at densities of 250 and 515 response units (RU), respectively, on the surfaces of two flow cells. Two-fold dilution series of TAB1 (0, 0.143, 0.285, 0.570, 1.14, 2.28, 4.56, 9.13, and 18.3 μM) and TAB1D (0, 0.203, 0.406, 0.813, 1.63, 3.25, 6.50, 13.0, and 26.0 μM) were tested in duplicate for binding to the surface-tethered XIAP proteins. The binding responses were double referenced (Myszka, 1999) and fit to a simple binding isotherm to determine affinity using Scrubber 2 (BioLogic Software Ltd., Campbell, Australia).

Crystallization and Structure Determination

The crystallization and structure determination of BIR1 will be described elsewhere. Briefly, BIR1 (residues 20–99) was crystallized in 1.5 M NaCl, 10% methanol, and 0.1 M HEPES at pH 7.5. The structure was determined at 1.8 Å resolution by single wavelength anomalous diffraction from the intrinsic Zn using Solve/Resolve (Terwilliger, 2004), auto-traced using ARP/wARP (Perrakis et al., 2001), and refined using CNS (Brunger et al., 1998) (Table 1). Human native and selenomethionyl TAB1 (residues 1–370) was crystallized in 1.5 M Li_2SO_4 and 0.1 M HEPES at pH 7.5. Multiwavelength anomalous diffraction data were collected at three wavelengths. The structure was determined at 2.6 Å resolution using Solve/Resolve (Terwilliger, 2004) and refined at 2.4 Å resolution against a native data set using CNS (Brunger et al., 1998). The final atomic model contains residues 18–370 (Table 1). TAB1D (residues 1–370 with deletion of 133–151) was mixed with excess BIR1 (residues 10–99) and subjected to gel filtration chromatography with Superdex 200 HR 26/60 (GE Biosciences). The BIR1/TAB1D complex peak was collected and concentrated to 20 mg/ml for crystallization under 8.5% PEG8000, 4% ethylene glycol, and 100 mM Na-HEPES at pH 7.6. The structure was determined at 3.1 Å resolution by molecular replacement (Tong, 1993) using the BIR1 and TAB1 structures (Table 1). Structural analysis was performed using O (Jones et al., 1991) and PyMOL (DeLano, 2002).

Knockdown of TAB1

Knockdown of TAB1 in MEFs was performed as previously described (Kang et al., 2006) Briefly, oligonucleotides were cloned into the vector pSuper to express short hairpin RNA; the targeting sequences are 5′-AGCAGTCCTTCTCAACAGCAAG-3′(#1) and 5′-AGGCCCTTCTGT GCAAATCTAC-3′ (#2). Cell lysates were prepared and subjected to western blot using anti-TAB1 or GAPDH antibodies. Total RNA was isolated, and semiquantitative PCR was performed.

NF-κB Activation by XIAP

293T cells, MEFs, or TAB1-knockdown MEFs (Kang et al., 2006) were transfected using Lipofectamine 2000 (Invitrogen) with NF-κB-luciferase, Renilla-luciferase (in pRT-TK using the herpes simplex virus thymidine kinase promoter, Promega), and control, full-length XIAP, or the following BIR1-3 domain expression vectors of XIAP: WT, V80D, or V86E. After 24 hr, cell lysates were prepared and luciferase activity was measured by luminometer. Fold activation of NF-κB was calculated by dividing measured luciferase activity of NF-κB by internal Renilla luciferase activity.

TAK1 Kinase Activity Assay

293 cells were transfected with 3 μg of an XIAP expression vector (control, WT full-length XIAP, WT, and mutant forms of XIAP BIR1-3) along with 1 μg of HA-TAK1 expression vector. After 24 hr, cell lysates were prepared in lysis buffer (20 mM HEPES [pH 7.4], 150 mM NaCl, 12.5 mM β-glycerophosphate, 1.5 mM $MgCl_2$, 2 mM EGTA, 10 mM NaF, 1 mM DTT, 1 mM Na_3VO_4, 1 mM PMSF, and 0.5% Triton X-100) and immunoprecipitated using anti-HA antibody for 3 hr. The immunoprecipitates were washed three times with lysis buffer and twice with kinase buffer (50 mM HEPES [pH 7.4], 1 mM dithiothreitol, 5 mM $MgCl_2$, and 50 μM ATP). They were incubated with 3 μg of kinase-dead MKK6 in kinase buffer containing 10 μCi of [γ-^{32}P]ATP at 37°C for 30 min. Two-thirds of the immunoprecipitates were subjected to SDS-PAGE and visualized by autoradiography, and the rest were subjected to western blot analysis to confirm the immunoprecipitation of HA-TAK1.

Dynamic Light Scattering

Hydrodynamic radius and estimated molecular mass of BIR1 at different concentrations were derived from dynamic light scattering measurements (Harding, 1994) on a DynoPro Molecular Sizing Instrument (Protein Solutions).

Supplemental Data

Supplemental Data include one figure and can be found with this article online at http://www.molecule.org/cgi/content/full/26/5/689/DC1/.

ACKNOWLEDGMENTS

We thank Dr. Colin Duckett and Arjmand Mufti for help with the project and providing the mammalian expression construct for WT BIR1-3 of XIAP, Dr. Yueming Li for providing the dimeric Smac peptide dAVPI, Jin Wu for maintaining X-ray and computer equipment, and Randy Abramowitz and John Schwanof for data collection at X4A and X4C of NSLS. This work was supported by the National Institute of Health (RO1 AI045937 to H.W., AI041637 and GM037696 to J.H.). M.L. is a postdoctoral fellow of the American Heart Association, and S.-C.L and Y.-C.L. are postdoctoral fellows of the Cancer Research Institute.

Received: January 10, 2007
Revised: April 3, 2007
Accepted: May 7, 2007
Published: June 7, 2007

REFERENCES

Andersen, M.H., Becker, J.C., and Straten, P. (2005). Regulators of apoptosis: suitable targets for immune therapy of cancer. Nat. Rev. Drug Discov. *4*, 399–409.

Berezovskaya, O., Schimmer, A.D., Glinskii, A.B., Pinilla, C., Hoffman, R.M., Reed, J.C., and Glinsky, G.V. (2005). Increased expression of apoptosis inhibitor protein XIAP contributes to anoikis resistance of circulating human prostate cancer metastasis precursor cells. Cancer Res. *65*, 2378–2386.

Birkey Reffey, S., Wurthner, J.U., Parks, W.T., Roberts, A.B., and Duckett, C.S. (2001). X-linked inhibitor of apoptosis protein functions as a cofactor in transforming growth factor-beta signaling. J. Biol. Chem. *276*, 26542–26549.

Brown, K., Vial, S.C., Dedi, N., Long, J.M., Dunster, N.J., and Cheetham, G.M. (2005). Structural basis for the interaction of TAK1 kinase with its activating protein TAB1. J. Mol. Biol. *354*, 1013–1020.

Brunger, A.T., Adams, P.D., Clore, G.M., DeLano, W.L., Gros, P., Grosse-Kunstleve, R.W., Jiang, J.S., Kuszewski, J., Nilges, M., Pannu, N.S., et al. (1998). Crystallography & NMR system: a new software suite for macromolecular structure determination. Acta Crystallogr. D Biol. Crystallogr. *54*, 905–921.

Chai, J., Du, C., Wu, J.W., Kyin, S., Wang, X., and Shi, Y. (2000). Structural and biochemical basis of apoptotic activation by Smac/DIABLO. Nature *406*, 855–862.

Chai, J., Shiozaki, E., Srinivasula, S.M., Wu, Q., Datta, P., Alnemri, E.S., Shi, Y., and Dataa, P. (2001). Structural basis of caspase-7 inhibition by XIAP. Cell *104*, 769–780.

Chawla-Sarkar, M., Bae, S.I., Reu, F.J., Jacobs, B.S., Lindner, D.J., and Borden, E.C. (2004). Downregulation of Bcl-2, FLIP or IAPs (XIAP and survivin) by siRNAs sensitizes resistant melanoma cells to Apo2L/TRAIL-induced apoptosis. Cell Death Differ. *11*, 915–923.

Chen, Z.J. (2005). Ubiquitin signalling in the NF-kappaB pathway. Nat. Cell Biol. *7*, 758–765.

Conner, S.H., Kular, G., Peggie, M., Shepherd, S., Schuttelkopf, A.W., Cohen, P., and Van Aalten, D.M. (2006). TAK1-binding protein 1 is a pseudophosphatase. Biochem. J. *399*, 427–434.

Crook, N.E., Clem, R.J., and Miller, L.K. (1993). An apoptosis-inhibiting baculovirus gene with a zinc finger-like motif. J. Virol. *67*, 2168–2174.

Das, A.K., Helps, N.R., Cohen, P.T., and Barford, D. (1996). Crystal structure of the protein serine/threonine phosphatase 2C at 2.0 Å resolution. EMBO J. *15*, 6798–6809.

DeLano, W.L. (2002). The PyMOL User's Manual (Palo Alto, CA: DeLano Scientific).

Deng, L., Wang, C., Spencer, E., Yang, L., Braun, A., You, J., Slaughter, C., Pickart, C., and Chen, Z.J. (2000). Activation of the IkappaB kinase complex by TRAF6 requires a dimeric ubiquitin-conjugating enzyme complex and a unique polyubiquitin chain. Cell *103*, 351–361.

Deveraux, Q.L., Takahashi, R., Salvesen, G.S., and Reed, J.C. (1997). X-linked IAP is a direct inhibitor of cell-death proteases. Nature *388*, 300–304.

Du, C., Fang, M., Li, Y., Li, L., and Wang, X. (2000). Smac, a mitochondrial protein that promotes cytochrome c-dependent caspase activation by eliminating IAP inhibition. Cell *102*, 33–42.

Duckett, C.S., Nava, V.E., Gedrich, R.W., Clem, R.J., Van Dongen, J.L., Gilfillan, M.C., Shiels, H., Hardwick, J.M., and Thompson, C.B. (1996). A conserved family of cellular genes related to the baculovirus iap gene and encoding apoptosis inhibitors. EMBO J. *15*, 2685–2694.

Eckelman, B.P., Salvesen, G.S., and Scott, F.L. (2006). Human inhibitor of apoptosis proteins: why XIAP is the black sheep of the family. EMBO Rep. *7*, 988–994.

Ferreon, J.C., and Hilser, V.J. (2004). Thermodynamics of binding to SH3 domains: the energetic impact of polyproline II (PII) helix formation. Biochemistry *43*, 7787–7797.

Harding, S.E. (1994). Determination of diffusion coefficients of biological macromolecules by dynamic light scattering. Methods Mol. Biol. *22*, 97–108.

Hay, B.A., Wassarman, D.A., and Rubin, G.M. (1995). Drosophila homologs of baculovirus inhibitor of apoptosis proteins function to block cell death. Cell *83*, 1253–1262.

Hofer-Warbinek, R., Schmid, J.A., Stehlik, C., Binder, B.R., Lipp, J., and de Martin, R. (2000). Activation of NF-kappa B by XIAP, the X chromosome-linked inhibitor of apoptosis, in endothelial cells involves TAK1. J. Biol. Chem. *275*, 22064–22068.

Holcik, M., Gibson, H., and Korneluk, R.G. (2001). XIAP: apoptotic brake and promising therapeutic target. Apoptosis *6*, 253–261.

Huang, Y., Park, Y.C., Rich, R.L., Segal, D., Myszka, D.G., and Wu, H. (2001). Structural basis of caspase inhibition by XIAP: differential roles of the linker versus the BIR domain. Cell *104*, 781–790.

Huang, Y., Rich, R.L., Myszka, D.G., and Wu, H. (2003). Requirement of both the second and third BIR domains for the relief of X-linked

inhibitor of apoptosis protein (XIAP)-mediated caspase inhibition by Smac. J. Biol. Chem. *278*, 49517–49522.

Jadrich, J.L., O'Connor, M.B., and Coucouvanis, E. (2003). Expression of TAK1, a mediator of TGF-beta and BMP signaling, during mouse embryonic development. Gene Expr. Patterns *3*, 131–134.

Jadrich, J.L., O'Connor, M.B., and Coucouvanis, E. (2006). The TGF beta activated kinase TAK1 regulates vascular development in vivo. Development *133*, 1529–1541.

Jones, T.A., Zou, J.-Y., Cowan, S.W., and Kjeldgaard, M. (1991). Improved methods for building models in electron density maps and the location of errors in those models. Acta Crystallogr. A *47*, 110–119.

Kanayama, A., Seth, R.B., Sun, L., Ea, C.K., Hong, M., Shaito, A., Chiu, Y.H., Deng, L., and Chen, Z.J. (2004). TAB2 and TAB3 activate the NF-kappaB pathway through binding to polyubiquitin chains. Mol. Cell *15*, 535–548.

Kang, Y.J., Seit-Nebi, A., Davis, R.J., and Han, J. (2006). Multiple activation mechanisms of p38alpha mitogen-activated protein kinase. J. Biol. Chem. *281*, 26225–26234.

Levkau, B., Garton, K.J., Ferri, N., Kloke, K., Nofer, J.R., Baba, H.A., Raines, E.W., and Breithardt, G. (2001). xIAP induces cell-cycle arrest and activates nuclear factor-kappaB: new survival pathways disabled by caspase-mediated cleavage during apoptosis of human endothelial cells. Circ. Res. *88*, 282–290.

Lewis, J., Burstein, E., Reffey, S.B., Bratton, S.B., Roberts, A.B., and Duckett, C.S. (2004). Uncoupling of the signaling and caspase-inhibitory properties of X-linked inhibitor of apoptosis. J. Biol. Chem. *279*, 9023–9029.

Liu, Z., Sun, C., Olejniczak, E.T., Meadows, R.P., Betz, S.F., Oost, T., Herrmann, J., Wu, J.C., and Fesik, S.W. (2000). Structural basis for binding of Smac/DIABLO to the XIAP BIR3 domain. Nature *408*, 1004–1008.

McManus, D.C., Lefebvre, C.A., Cherton-Horvat, G., St-Jean, M., Kandimalla, E.R., Agrawal, S., Morris, S.J., Durkin, J.P., and Lacasse, E.C. (2004). Loss of XIAP protein expression by RNAi and antisense approaches sensitizes cancer cells to functionally diverse chemotherapeutics. Oncogene *23*, 8105–8117.

Mufti, A.R., Burstein, E., Csomos, R.A., Graf, P.C., Wilkinson, J.C., Dick, R.D., Challa, M., Son, J.K., Bratton, S.B., Su, G.L., et al. (2006). XIAP Is a copper binding protein deregulated in Wilson's disease and other copper toxicosis disorders. Mol. Cell *21*, 775–785.

Myszka, D.G. (1999). Improving biosensor analysis. J. Mol. Recognit. *12*, 279–284.

Nagar, B., Hantschel, O., Young, M.A., Scheffzek, K., Veach, D., Bornmann, W., Clarkson, B., Superti-Furga, G., and Kuriyan, J. (2003). Structural basis for the autoinhibition of c-Abl tyrosine kinase. Cell *112*, 859–871.

Olayioye, M.A., Kaufmann, H., Pakusch, M., Vaux, D.L., Lindeman, G.J., and Visvader, J.E. (2005). XIAP-deficiency leads to delayed lobuloalveolar development in the mammary gland. Cell Death Differ. *12*, 87–90.

Park, Y.C., Burkitt, V., Villa, A.R., Tong, L., and Wu, H. (1999). Structural basis for self-association and receptor recognition of human TRAF2. Nature *398*, 533–538.

Pato, M.D., and Kerc, E. (1991). Regulation of smooth muscle phosphatase-II by divalent cations. Mol. Cell. Biochem. *101*, 31–41.

Perrakis, A., Harkiolaki, M., Wilson, K.S., and Lamzin, V.S. (2001). ARP/wARP and molecular replacement. Acta Crystallogr. D Biol. Crystallogr. *57*, 1445–1450.

Pullen, K.E., Ng, H.L., Sung, P.Y., Good, M.C., Smith, S.M., and Alber, T. (2004). An alternate conformation and a third metal in PstP/Ppp, the M. tuberculosis PP2C-family Ser/Thr protein phosphatase. Structure *12*, 1947–1954.

Riedl, S.J., Renatus, M., Schwarzenbacher, R., Zhou, Q., Sun, C., Fesik, S.W., Liddington, R.C., and Salvesen, G.S. (2001). Structural basis for the inhibition of caspase-3 by XIAP. Cell *104*, 791–800.

Rothe, M., Pan, M.G., Henzel, W.J., Ayres, T.M., and Goeddel, D.V. (1995). The TNFR2-TRAF signaling complex contains two novel proteins related to baculoviral inhibitor of apoptosis proteins. Cell *83*, 1243–1252.

Samuel, T., Welsh, K., Lober, T., Togo, S.H., Zapata, J.M., and Reed, J.C. (2006). Distinct BIR domains of cIAP1 mediate binding to and ubiquitination of tumor necrosis factor receptor-associated factor 2 and second mitochondrial activator of caspases. J. Biol. Chem. *281*, 1080–1090.

Sanna, M.G., Duckett, C.S., Richter, B.W., Thompson, C.B., and Ulevitch, R.J. (1998). Selective activation of JNK1 is necessary for the anti-apoptotic activity of hILP. Proc. Natl. Acad. Sci. USA *95*, 6015–6020.

Sanna, M.G., da Silva Correia, J., Ducrey, O., Lee, J., Nomoto, K., Schrantz, N., Deveraux, Q.L., and Ulevitch, R.J. (2002). IAP suppression of apoptosis involves distinct mechanisms: the TAK1/JNK1 signaling cascade and caspase inhibition. Mol. Cell. Biol. *22*, 1754–1766.

Sasaki, H., Sheng, Y., Kotsuji, F., and Tsang, B.K. (2000). Down-regulation of X-linked inhibitor of apoptosis protein induces apoptosis in chemoresistant human ovarian cancer cells. Cancer Res. *60*, 5659–5666.

Schimmer, A.D., Dalili, S., Batey, R.A., and Riedl, S.J. (2006). Targeting XIAP for the treatment of malignancy. Cell Death Differ. *13*, 179–188.

Shibuya, H., Yamaguchi, K., Shirakabe, K., Tonegawa, A., Gotoh, Y., Ueno, N., Irie, K., Nishida, E., and Matsumoto, K. (1996). TAB1: an activator of the TAK1 MAPKKK in TGF-beta signal transduction. Science *272*, 1179–1182.

Shibuya, H., Iwata, H., Masuyama, N., Gotoh, Y., Yamaguchi, K., Irie, K., Matsumoto, K., Nishida, E., and Ueno, N. (1998). Role of TAK1 and TAB1 in BMP signaling in early Xenopus development. EMBO J. *17*, 1019–1028.

Shiozaki, E.N., Chai, J., Rigotti, D.J., Riedl, S.J., Li, P., Srinivasula, S.M., Alnemri, E.S., Fairman, R., and Shi, Y. (2003). Mechanism of XIAP-mediated inhibition of caspase-9. Mol. Cell *11*, 519–527.

Silke, J., Hawkins, C.J., Ekert, P.G., Chew, J., Day, C.L., Pakusch, M., Verhagen, A.M., and Vaux, D.L. (2002). The anti-apoptotic activity of XIAP is retained upon mutation of both the caspase 3- and caspase 9-interacting sites. J. Cell Biol. *157*, 115–124.

Silke, J., Kratina, T., Chu, D., Ekert, P.G., Day, C.L., Pakusch, M., Huang, D.C., and Vaux, D.L. (2005). Determination of cell survival by RING-mediated regulation of inhibitor of apoptosis (IAP) protein abundance. Proc. Natl. Acad. Sci. USA *102*, 16182–16187.

Takaesu, G., Kishida, S., Hiyama, A., Yamaguchi, K., Shibuya, H., Irie, K., Ninomiya-Tsuji, J., and Matsumoto, K. (2000). TAB2, a novel adaptor protein, mediates activation of TAK1 MAPKKK by linking TAK1 to TRAF6 in the IL-1 signal transduction pathway. Mol. Cell *5*, 649–658.

Takatsu, Y., Nakamura, M., Stapleton, M., Danos, M.C., Matsumoto, K., O'Connor, M.B., Shibuya, H., and Ueno, N. (2000). TAK1 participates in c-Jun N-terminal kinase signaling during Drosophila development. Mol. Cell. Biol. *20*, 3015–3026.

Tang, E.D., Wang, C.Y., Xiong, Y., and Guan, K.L. (2003). A role for NF-kappaB essential modifier/IkappaB kinase-gamma (NEMO/IKKgamma) ubiquitination in the activation of the IkappaB kinase complex by tumor necrosis factor-alpha. J. Biol. Chem. *278*, 37297–37305.

Terwilliger, T. (2004). SOLVE and RESOLVE: automated structure solution, density modification and model building. J. Synchrotron Radiat. *11*, 49–52.

Tong, L. (1993). REPLACE, a suite of computer programs for molecular-replacement calculations. J. Appl. Crystallogr. *26*, 748–751.

Tong, Q.S., Zheng, L.D., Wang, L., Zeng, F.Q., Chen, F.M., Dong, J.H., and Lu, G.C. (2005). Downregulation of XIAP expression induces apoptosis and enhances chemotherapeutic sensitivity in human gastric cancer cells. Cancer Gene Ther. *12*, 509–514.

Varfolomeev, E., Wayson, S.M., Dixit, V.M., Fairbrother, W.J., and Vucic, D. (2006). The inhibitor of apoptosis protein fusion c-IAP2. MALT1 stimulates NF-kappaB activation independently of TRAF1 AND TRAF2. J. Biol. Chem. *281*, 29022–29029.

Vaux, D.L., and Silke, J. (2005). IAPs, RINGs and ubiquitylation. Nat. Rev. Mol. Cell Biol. *6*, 287–297.

Verhagen, A.M., Ekert, P.G., Pakusch, M., Silke, J., Connolly, L.M., Reid, G.E., Moritz, R.L., Simpson, R.J., and Vaux, D.L. (2000). Identification of DIABLO, a mammalian protein that promotes apoptosis by binding to and antagonizing IAP proteins. Cell *102*, 43–53.

Wang, C., Deng, L., Hong, M., Akkaraju, G.R., Inoue, J., and Chen, Z.J. (2001). TAK1 is a ubiquitin-dependent kinase of MKK and IKK. Nature *412*, 346–351.

Wilkinson, J.C., Cepero, E., Boise, L.H., and Duckett, C.S. (2004). Upstream regulatory role for XIAP in receptor-mediated apoptosis. Mol. Cell. Biol. *24*, 7003–7014.

Wu, H., Kwong, P.D., and Hendrickson, W.A. (1997). Dimeric association and segmental variability in the structure of human CD4. Nature *387*, 527–530.

Wu, G., Chai, J., Suber, T.L., Wu, J.W., Du, C., Wang, X., and Shi, Y. (2000). Structural basis of IAP recognition by Smac/DIABLO. Nature *408*, 1008–1012.

Yamaguchi, K., Shirakabe, K., Shibuya, H., Irie, K., Oishi, I., Ueno, N., Taniguchi, T., Nishida, E., and Matsumoto, K. (1995). Identification of a member of the MAPKKK family as a potential mediator of TGF-beta signal transduction. Science *270*, 2008–2011.

Yamaguchi, K., Nagai, S., Ninomiya-Tsuji, J., Nishita, M., Tamai, K., Irie, K., Ueno, N., Nishida, E., Shibuya, H., and Matsumoto, K. (1999). XIAP, a cellular member of the inhibitor of apoptosis protein family, links the receptors to TAB1-TAK1 in the BMP signaling pathway. EMBO J. *18*, 179–187.

Ye, H., Arron, J.R., Lamothe, B., Cirilli, M., Kobayashi, T., Shevde, N.K., Segal, D., Dzivenu, O.K., Vologodskaia, M., Yim, M., et al. (2002). Distinct molecular mechanism for initiating TRAF6 signalling. Nature *418*, 443–447.

Zhou, H., Du, M.Q., and Dixit, V.M. (2005). Constitutive NF-kappaB activation by the t(11;18)(q21;q21) product in MALT lymphoma is linked to deregulated ubiquitin ligase activity. Cancer Cell *7*, 425–431.

Accession Numbers

The coordinates have been deposited in the RCSB Protein Data Bank with the PDB codes of 2POP for the BIR1/TAB1 structure, 2POI for the BIR1 structure, and 2POM for the structure of Mn^{2+}-soaked TAB1.

Molecular Cell, Volume *26*

Supplemental Data

XIAP Induces NF-κB Activation via the BIR1/TAB1 Interaction and BIR1 Dimerization

Miao Lu, Su-Chang Lin, Yihua Huang, Young Jun Kang, Rebecca Rich, Yu-Chih Lo, David Myszka, Jiahuai Han, and Hao Wu

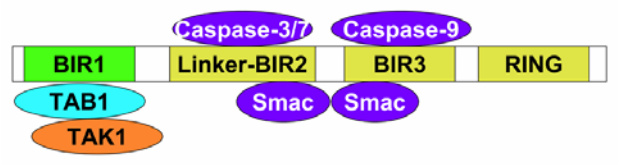

Figure S1. Domain Organization of XIAP and Its Interacting Partners